

Pollinators contribute to the maintenance of flowering plant diversity

<https://doi.org/10.1038/s41586-021-03890-9>

Received: 17 September 2020

Accepted: 9 August 2021

Published online: 08 September 2021

 Check for updates

Na Wei^{1,2✉}, Rainee L. Kaczorowski¹, Gerardo Arceo-Gómez^{1,3}, Elizabeth M. O'Neill¹, Rebecca A. Hayes¹ & Tia-Lynn Ashman^{1✉}

Mechanisms that favour rare species are key to the maintenance of diverse communities^{1–3}. One of the most critical tasks for conservation of flowering plant biodiversity is to understand how plant–pollinator interactions contribute to the maintenance of rare species^{4–7}. Here we show that niche partitioning in pollinator use and asymmetric facilitation confer fitness advantage of rarer species in a biodiversity hotspot using phylogenetic structural equation modelling that integrates plant–pollinator and interspecific pollen transfer networks with floral functional traits. Co-flowering species filtered pollinators via floral traits, and rarer species showed greater pollinator specialization leading to higher pollination-mediated male and female fitness than more abundant species. When plants shared pollinator resources, asymmetric facilitation via pollen transport dynamics benefitted the rarer species at the cost of more abundant species, serving as an alternative diversity-promoting mechanism. Our results emphasize the importance of community-wide plant–pollinator interactions that affect reproduction for biodiversity maintenance.

How numerous rare species coexist with abundant species is a major unresolved question in ecology but is essential to understanding the maintenance of species diversity^{1,2}. Plant–pollinator interactions are thought to be among the most important drivers of biodiversity on Earth⁴ but points of controversy remain⁸. Evidence suggests that the great majority of flowering plants (approximately 80%) are pollinated by animals⁹, and that without pollinators more than half would suffer marked declines in seed production despite the fact that most have the capability for autofertility¹⁰. Yet, we still lack a clear view as to how community-wide interactions between plants and pollinators may contribute to the persistence of rare plant species that are at greater risk of extinction than abundant species^{11–13}. Mechanisms such as niche partitioning³ and facilitation¹⁴ can help to maintain rare species. Niche partitioning can prevent interspecific competitive exclusion between rare and abundant species. Conversely, facilitation generates positive interspecific interactions. Evidence suggests that both mechanisms can operate at the pollination stage of the plant life cycle and may confer a pollination-mediated fitness advantage to rare species over abundant species^{15–17}, but the relative importance of these mechanisms in natural communities with numerous coexisting flowering plant species remains to be elucidated.

Tracking pollination-mediated fitness in diverse plant communities is more complex than tracking fitness at later life stages (for example, seed production or seedling growth). Because most plants are hermaphrodites¹⁸, fitness at the pollination stage has both female and male components (via ovules that house eggs and pollen that houses sperm). Thus, fitness gain is only achieved from a female–male interaction when pollen from conspecific donors reaches conspecific ovules. The receipt of conspecific pollen (CP) per ovule can therefore reflect this joint fitness gain mediated by pollinators, when seed production

is limited by the amount of pollen and male fitness is limited by the number of ovules. By contrast, when the pollen received is from another plant species (that is, receipt of heterospecific pollen (HP)), loss of fitness can occur. Specifically, HP can reduce female fitness by clogging stigmas or usurping ovules¹⁹. Likewise, interference of HP with legitimate pollen (CP) can reduce the success of siring. Loss of fitness can also occur when pollinators misdeliver pollen, that is, transport it to heterospecific rather than conspecific plants (misplacement of CP)²⁰. Such transfer lowers siring opportunities. Under pollen-limited conditions, CP misplacement or loss during transport can also lower female fitness. Given the multiple pathways of fitness accrual via complex plant–pollinator interactions, a community-wide study is required to assess how components of pollinator-mediated fitness combine to potentially contribute to the maintenance of rare plant species; yet, no such study exists.

As pollinator service is often limited in nature²¹, competition for successful pollination predicts limiting similarity in pollinator sharing¹². Because of fitness costs associated with generalization, niche partitioning of pollinators can potentially favour rare plant species via their greater specialization than abundant species. In a diverse co-flowering plant community (Fig. 1a, Table 1, H1), the cost of being a generalist plant includes high risks of fitness loss due to misplacement of CP and receipt of HP, which can reduce joint fitness gain¹⁹. By contrast, the benefit of being a specialist plant may include improved delivery of CP by pollinators and lower risks of fitness loss, provided that there is adequate visitation.

However, when pollinator niches overlap, asymmetric facilitation can favour rare plant species^{17,22} (Fig. 1b, Table 1, H2). Rare species benefit from pollinators being attracted by abundant heterospecific neighbours¹⁷. Although rare species may also receive HP when sharing

¹Department of Biological Sciences, University of Pittsburgh, Pittsburgh, PA, USA. ²The Holden Arboretum, Kirtland, OH, USA. ³Department of Biological Sciences, East Tennessee State University, Johnson City, TN, USA. ✉e-mail: nwei@holdenfg.org; tial1@pitt.edu

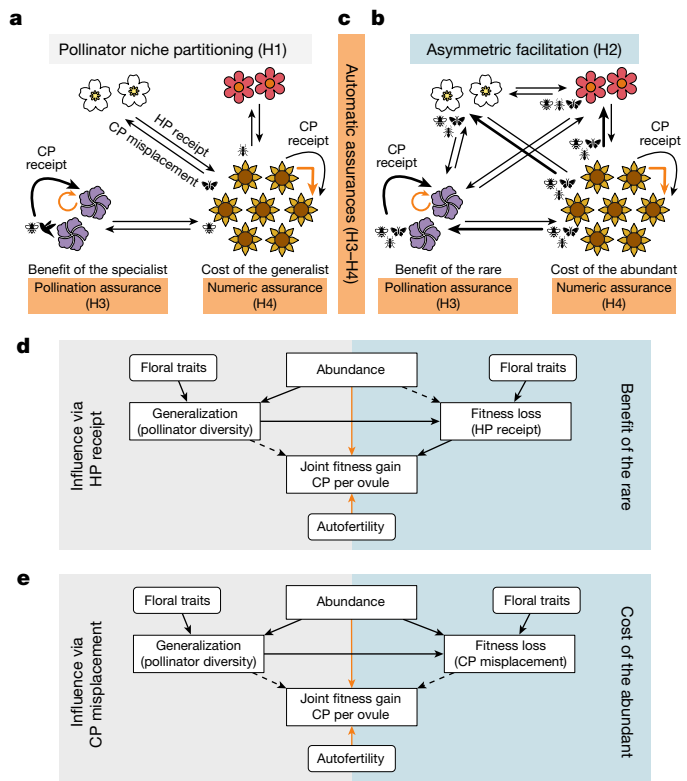


Fig. 1 | Schematic framework of how pollinator niche partitioning, asymmetric facilitation and automatic assurances confer rare species advantage. **a**, Pollinator niche partitioning occurs when plants (flower icons) use different sets of pollinators (insect icons). Generalist plants (for example, yellow flowers) by virtue of sharing pollinators with other species (for example, red, white and purple flowers) experience higher risks of misplacement of CP (more outgoing arrows) and receipt of HP (more incoming arrows), two processes that potentially lead to fitness losses. By contrast, specialist plants (for example, purple flowers) that were visited by fewer shared pollinators benefit from higher delivery of CP (thickened curved arrow) and lower risks of fitness losses via misplacement of CP and receipt of HP, provided there was adequate visitation. Thus, niche partitioning can favour rare plant species via greater specialization relative to abundant species. **b**, When sharing pollinator niches, abundant species (yellow flowers) experience higher misplacement of CP (thickened outgoing arrows) when pollinators that primarily visit them move to rare species (red, white and purple flowers). In turn, rare species benefit from pollinators attracted by abundant species, leading to greater receipt of CP than if they were growing alone. **c**, Automatic assurances include ‘pollination assurance’ of CP delivery via autonomous self-pollination (the orange circular arrow of the purple flowers in **a** and **b**), which can benefit rare (purple) species even if abundant (yellow) species have the intrinsic numeric advantage (‘numeric assurance’; the orange angled arrow of the yellow flowers in **a** and **b**) of receiving mainly CP by virtue of their high abundance. **d, e**, These mechanisms can be examined by linking pollinator niche breadth (generalization), plant rarity (abundance) and autofertility via autonomous self-pollination to fitness gain and loss due to receipt of HP (**d**) and misplacement of CP (**e**). The black and orange arrows indicate positive (solid) and negative (dashed) relationships between factors that are involved in pathways of causation for each hypothesis (Table 1): pollinator niche partitioning (H1, black arrows), asymmetric facilitation (H2, black arrows), pollination assurance (H3, orange arrow) and numeric assurance (H4, orange arrow).

pollinators with abundant species²³, they can receive more CP than they would if growing alone. Thus, a positive relationship between receipt of HP and CP can reflect the relative strength of this facilitation^{22,41} (see ref. ²⁴ for caveats). Likewise, abundant species, as facilitators, may experience more misplacement of CP to heterospecific plants than they would if growing without the rare species. Thus, asymmetric

facilitation can potentially increase the joint fitness gain of rare species but decrease that of abundant species due to fitness losses of CP misplacement.

In contrast to pollinator-mediated mechanisms, rare species can potentially be maintained by autofertility. Autonomous self-pollination is a mechanism of autofertility where pollen transfer from anther to stigma occurs within a flower without the aid of a pollinator. Deposition of self-pollen is more likely when there is only a small physical distance between stigmas and anthers¹⁸. Thus, autonomous self-pollination is a reproductive assurance mechanism that is beneficial when the availability of pollinators and/or mates is low²⁵. As a result, autofertility may increase joint fitness gain and retain rare species²³ (Fig. 1c, Table 1, H3), even when a presumed numeric advantage of abundance exists, that is, abundant species mainly receive CP simply by virtue of their high abundance and irrespective of which pollinator visits²⁶ (Fig. 1c, Table 1, H4).

Functional trait divergence among species that share pollinator resources is predicted to assist their coexistence²⁷. In particular, floral traits related to pollinator attraction and mechanical fit are important for filtering pollinators and thus mediating the pollinator niche of plants²⁸. Floral traits related to the female and male reproductive organs (for example, stigma and stamen features, respectively) influence pollen receipt and donation^{19,29}. However, evidence linking these floral traits to differences in pollinator niche³⁰, fitness losses via receipt of HP³¹ or misplacement of CP⁴¹, and joint fitness gain beyond pairs of interacting species is rare and virtually nonexistent across entire interaction networks in species-rich communities. This is perhaps due to the challenges of recording pollination-mediated fitness of all the taxa in these communities, especially identifying and tracking misdelivered pollen grains²⁰. Thus, the combinations of traits that govern pollinator diversity and fitness differences among plant species, and thereby modulate the strength of niche partitioning and facilitation or pollination assurance, remain entirely unknown in the very communities where we expect these processes to be the strongest: high-diversity ecosystems such as global biodiversity hotspots.

Here we evaluated the mechanisms that have been hypothesized to underlie advantage in rare species, along with potential functional trait drivers, in a global biodiversity hotspot³²: the serpentine seep communities of the grassland/scrub habitats of California, USA. We formulated a modelling framework (Fig. 1d, e, Table 1) to describe the relationships among floral traits and pathways for fitness gains and losses associated with pollinator niche breadth (generalization) and plant species rarity (abundance), and in the context of pollination assurance (autofertility) and numeric assurance, across all the species in the co-flowering community. To assess the hypothesis of rare species advantage due to pollinator niche partitioning, we first tested whether plant species are limited in sharing of pollinators. We then asked whether rarer plant species are more specialized, thus leading to higher joint fitness gain, than more abundant species (as a result of net negative effects of H1.1–H1.3) (Table 1, Fig. 1d, e). To assess the hypothesis of asymmetric facilitation (Table 1, H2), we asked whether rarer species are facilitated more than more abundant species by receiving more CP (along with more HP), leading to increased joint fitness gain (Table 1, H2.1, Fig. 1d). In turn, we asked whether more abundant species, as facilitators, experience higher fitness loss via misplacement of CP, leading to reduced joint fitness gain relative to rarer species (Table 1, H2.2, Fig. 1e). To assess the pollination assurance hypothesis, we asked whether a shorter stigma–anther distance (a trait that encourages deposition of self-pollen and autofertility)¹⁸ leads to higher joint fitness gain (Table 1, H3), and whether rarer species possess shorter stigma–anther distances. We tested the pollination assurance hypothesis along with the pollinator-mediated mechanisms, as well as the presumed numeric assurance associated with greater abundance²⁶ (Table 1, H4). Numeric assurance was explicitly tested by linking abundance directly to joint fitness gain (Fig. 1d, e). These hypotheses were examined using phylogenetic structural equation

Table 1 | Hypotheses of pollination-mediated maintenance of rare species

Hypotheses	Mechanisms	Pathways ^a
H1: pollinator niche partitioning	(1) Abundant species support more pollinators (more generalized), which can decrease CP per ovule due to greater pollen consumption or loss	H1.1: abundance → ⊕ pollinator diversity → ⊖ CP per ovule
	(2) Rarer species receive less HP due to more specialized pollinators. Yet, the effect of HP on CP per ovule can be positive due to co-transport of CP and HP, and deposition of CP is mediated by the pollinator as indicated by delivery of HP	H1.2: abundance → ⊕ pollinator diversity → ⊕ receipt of HP → ⊕ CP per ovule
	(3) Rarer species experience less misplacement of CP due to more specialized pollinators, leading to higher CP per ovule	H1.3: abundance → ⊕ pollinator diversity → ⊕ misplacement of CP → ⊖ CP per ovule
H2: asymmetric facilitation	(1) When sharing pollinators, rarer species receive more HP. This can increase CP per ovule due to increased deposition of CP accompanying pollinator visits that deliver HP	H2.1: abundance → ⊖ receipt of HP → ⊕ CP per ovule
	(2) When sharing pollinators, abundant species experience higher misplacement of CP when pollinators that primarily visit abundant species move to rarer species. This can lower CP per ovule	H2.2: abundance → ⊕ misplacement of CP → ⊖ CP per ovule
H3: pollination assurance	Autonomous self-pollination leads to higher CP per ovule directly	Autofertility → ⊕ CP per ovule
H4: numeric assurance	Abundance leads to higher CP per ovule directly	Abundance → ⊕ CP per ovule

Pollinator niche partitioning is the limiting similarity in pollinator sharing among plant species. The pollinator niche of a plant species is a set of animal species that visit and effectively pollinate the plant relative to the total pool of available pollinators. When plants are visited by different sets of pollinators, they partition pollinator niches. Asymmetric facilitation is a positive species interaction where the benefits are not equal among interacting species. Here coexistence with abundant species leads to more benefits for rare species, relative to abundant species that act as facilitators for pollinator attraction. Pollination assurance is the assurance of pollination even in the absence of pollinator visitation and/or conspecific mates. It is often mediated by autofertility mechanisms such as autonomous self-pollen deposition. Numeric assurance is the result of numerically dominant species receiving more CP simply by virtue of high abundance. ⊕ and ⊖ indicate positive and negative relationships, respectively. ^aPathways are shown in Fig. 1d, e.

modelling (PSEM) at two levels: (1) nested model selection was used to validate the inclusion of a hypothesized mechanism; and (2) paths within the selected models were used to assess the relative strength of hypothesized pathways. Our PSEM leveraged species-specific metrics derived from community-wide plant–pollinator and interspecific pollen transfer networks, and a suite of floral traits.

We observed plant–pollinator interactions during two consecutive flowering seasons in a system of serpentine seeps (10,000 m²) at the McLaughlin Natural Reserve (38.8582°N, 122.4093°W) (Extended Data Table 1). Among the 7,324 pollinators that visited 79 co-flowering plant species (of 62 genera from 29 families) (Extended Data Fig. 1), 416 species were identified (Supplementary Table 1): 192 bees ($n = 4,951$ individuals, Hymenoptera), 131 flies ($n = 1,409$, Diptera), 35 beetles ($n = 428$, Coleoptera), 30 butterflies and moths ($n = 244$, Lepidoptera), 14 wasps ($n = 104$, Hymenoptera), 3 ants ($n = 22$, Hymenoptera), 10 other insect species ($n = 25$) and 1 hummingbird species ($n = 141$, Trochilidae). The plant–pollinator network (Extended Data Fig. 1), based on sufficient field observations (Extended Data Fig. 2), revealed substantial variation in pollinator niche breadth among plant species, ranging from a plant interacting with 1 to 77 pollinator species (mean = 23). In contrast to the nested structure of many ecological networks³³ where specialist

plants share and interact with only subsets of the partners of generalist plants, the network was significantly less nested and more modular than random expectations (Methods; Supplementary Table 2), reducing pollinator sharing. These plants that flowered largely simultaneously (Supplementary Table 3) showed significantly less niche overlap (Horn's index = 0.086, null mean = 0.412, two-sided $P < 0.001$) and fewer shared pollinator partners (observed mean = 3, null mean = 17, $P < 0.001$) than expected by chance. For individual plant species, the majority (85%) exhibited significantly higher degrees of specialization than random expectations (Supplementary Table 2). As hypothesized, rarer species were more specialized than more abundant species (PSEM, $r = 0.42$, two-sided bootstrap $P < 0.05$) (Fig. 2). Overall, these plant–pollinator interactions strongly demonstrate differences in pollinator niche among coexisting plants.

To link functional traits to differences in pollinator niche, we scored 20 floral traits (Supplementary Table 3), revealing substantial phenotypic variation among coexisting plants independent of abundance (Extended Data Fig. 3). We categorized these traits by function, that is, pollinator attraction (Extended Data Fig. 4), and male (Extended Data Fig. 5) and female (Extended Data Fig. 6) organs, and performed multivariate analyses to obtain independent dimensions of trait variation within each group. We found multiple trait dimensions that reflected floral advertisement and mechanical fit to promote differences in pollinator niche among coexisting plants (Fig. 2). Specifically, the degree of pollination generalization, which was evolutionarily labile (Pagel's $\lambda = 0.075$, $P = 0.50$; Supplementary Table 4), was predicted by the first two dimensions of attraction traits ('Dim' 1–2, PSEM, $r = 0.43$ and -0.25 , respectively, $P < 0.05$) (Fig. 2); that is, species with open, funnellform (Dim 1) or aster-shaped (Dim 2) flowers were more generalized than pea (Dim 1) or salverform (Dim 2) flowers. Flower symmetry also predicted pollinator niche, with bilateral flowers more specialized than radial flowers (Extended Data Fig. 4), probably due to mechanical fit of pollinators²⁸. Similarly, longer flower tubes that filter pollinators by tongue length²⁸ were associated with less generalization. In contrast to these floral traits, male organ traits that potentially signal pollen rewards did not predict pollinator niche (Methods).

To track fitness at the pollination stage in the community, we taxonomically identified 3.1 million pollen grains that were deposited on stigmas of co-flowering species ($n = 54$ stigmas each of 66 species; Supplementary Table 5), over the 2 years of pollinator observations. We quantified fitness loss via misplacement of CP (delivered to coexisting heterospecific plants) and receipt of HP from the community-wide pollen transfer network (Extended Data Fig. 7), based on sufficient stigma sampling (Extended Data Fig. 8).

Nested model selection showed that the model considering pollinator niche partitioning and asymmetric facilitation alone often received the best support (Extended Data Fig. 9, Supplementary Table 6). When assessing mechanisms via receipt of HP (Fig. 1d), the model of pollinator niche partitioning and asymmetric facilitation was best supported (with the lowest C statistic information criterion) (Extended Data Fig. 9). Yet, the competing model that also included numeric assurance could not be rejected (Extended Data Fig. 9), and thus the model-averaged path diagram is presented (Fig. 2a). When assessing mechanisms via misplacement of CP (Fig. 1e), the model of pollinator niche partitioning and asymmetric facilitation was best supported (Fig. 2b, Extended Data Fig. 9). Model selection rejected the hypotheses of numeric assurance and pollination assurance (Extended Data Fig. 9). We further found that rarer species possessed longer stigma–anther distances that discourage self-pollination¹⁸ than more abundant species (phylogenetic generalized least-squares model (PGLS); $\chi^2 = 8.17$, d.f. = 1, two-sided $P = 0.004$). This result refutes a role for autonomous self-pollination in favouring rarer species in this community that has high pollinator diversity.

Using the averaged or best-supported model (Fig. 2a, b, respectively), we assessed the relative strength and sign of paths associated with supported hypotheses. For the pollinator niche partitioning hypothesis

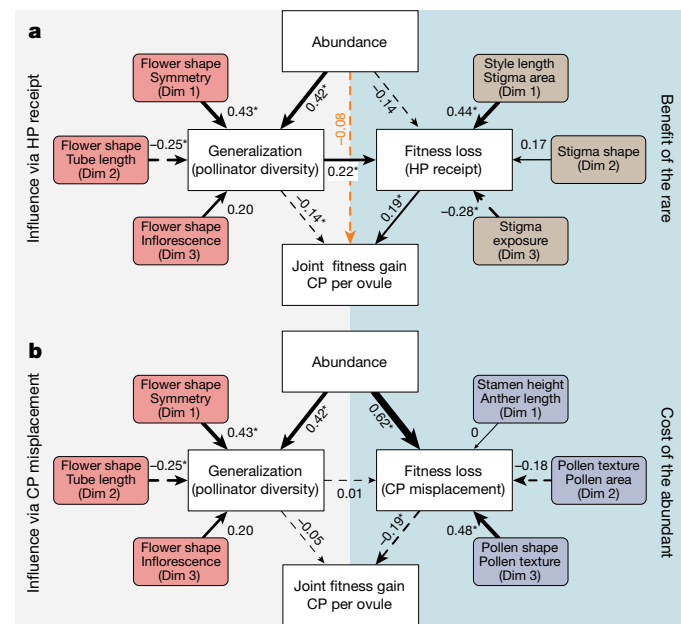


Fig. 2 | Plant–pollinator interactions favour rare species through pollinator niche partitioning and asymmetric facilitation, which are mediated by floral traits. a, b The results of PSEM demonstrate how pollinator niche breadth (generalization) and plant rarity (abundance) affect fitness loss via receipt of HP (a) and misplacement of CP (b) and thus joint fitness gain. After model selection to identify the single best-supported or average of the top models (Extended Data Fig. 9, Supplementary Table 6), the best path diagram models are presented ($n = 64$ plant species; Fisher’s $C = 30.8$, d.f. = 26, $P = 0.236$ (a); Fisher’s $C = 32.0$, d.f. = 26, $P = 0.195$ (b)); Source Data). Significant positive (solid arrows) and negative (dashed arrows) relationships between factors are indicated with asterisks (two-sided bootstrap $P \leq 0.05$). The arrow widths depict the effect sizes (standardized coefficients, r) of these relationships. The strength and sign of net effects of causal paths associated with hypotheses (Table 1) are calculated as the product of the standardized coefficients along the paths, which indicate one standard deviation change of a predictor leading to an r unit standard deviation change of a response variable (see Supplementary Notes for unstandardized net effects). The orange arrow indicates numeric assurance as in Fig. 1d. Floral attraction traits (red), and female (brown) and male (purple) organ traits are indicated, where ‘Dim’ indicates the multivariate dimension from factor analysis (Extended Data Figs. 4–6).

(Table 1, H1), we found that pollinator niche mediated fitness costs, with generalist plants receiving more HP and thus had the potential for higher fitness loss than specialist plants ($r = 0.22$, $P < 0.05$) (Fig. 2a), which is in line with previous studies^{31,41}. Although the co-transport and receipt of HP–CP^{22,41} contributed positively ($r = 0.19$, $P < 0.05$) (Fig. 2a) to joint fitness gain (CP per ovule), pollinator diversity directly reduced joint fitness gain ($r = -0.14$, $P = 0.05$), possibly due to pollen consumption or other mechanisms of pollen loss during transport²⁹. As a result, there was a net negative fitness effect of generalization ($r = -0.10$ ($-0.14 + 0.22 \times 0.19$)) (Fig. 2a, Supplementary Notes: 24% reduction in CP per ovule with a one unit increase in generalization), in line with the niche partitioning hypothesis. Thus, in support of rare species advantage mediated by pollinator niche differentiation (Fig. 1d, Table 1, H1), we found that rarer species were more specialized and thus had higher net joint fitness gain (net effect of abundance: $r = -0.04$ ($0.42 \times -0.14 + 0.42 \times 0.22 \times 0.19$)) (Fig. 2a, Supplementary Notes: 19% reduction in CP per ovule with a 100-fold increase in floral abundance). Generalization, however, showed no direct effect on pollen misplacement ($r = 0.01$, $P > 0.05$) (Fig. 2b), which is in contrast to our hypothesis that it would lead to higher fitness loss (Fig. 1e, Table 1, H1.3). This suggests that pollinator diversity and visit quantity¹³ are perhaps less important than other factors such as pollinator quality in mediating misplacement of

pollen to heterospecific plants. Together, these results demonstrate a measurable fitness cost of species abundance via generalization in the supported models.

To assess the strength of asymmetric facilitation, we differentiated abundance-based causes from trait-based causes of fitness differences among coexisting plants (Fig. 2). We found that traits of the female organ mediated fitness loss via receipt of HP (Fig. 2a), whereas traits of the male organ influenced fitness loss via misplacement of CP (Fig. 2b). Larger stigmas and longer styles ($r = 0.44$, $P < 0.05$) (Fig. 2a) or stigmas that did not extend beyond the corolla ($r = -0.28$, $P < 0.05$) led to higher receipt of HP. Pollen morphology explained a substantial amount of variation among species in CP misplacement ($r = 0.48$, $P < 0.05$, Dim3) (Fig. 2b). Textured (for example, spiky or granulate) or regular-shaped (for example, round) pollen was more likely to be misplaced (that is, deposited on heterospecific plants) than smooth or irregular-shaped pollen. After accounting for the influence of floral traits, we isolated abundance-dependent effects on pollen transport and pollinator-mediated fitness and revealed evidence for facilitation. In line with the asymmetric facilitation hypothesis (Fig. 1d, Table 1, H2.1), rarer species tended to receive slightly more HP from coexisting heterospecific plants than more abundant species ($r = -0.14$) (Fig. 2a). Yet, pollinators that delivered HP also enhanced delivery of CP^{22,41}, contributing to a positive effect on joint fitness gain ($r = 0.19$, $P < 0.05$) (Fig. 2a), which led to a greater benefit for rarer species (or greater cost for more abundant species; $r = -0.03$ (-0.14×0.19)) (Supplementary Notes: 15% reduction in CP per ovule with a 100-fold increase in floral abundance). In addition, higher abundance led to greater fitness loss via misplacement of CP ($r = 0.62$, $P < 0.05$) (Fig. 2b), which translated into lowered joint fitness gain for more abundant species ($r = -0.12$ (0.62×-0.19)) (Supplementary Notes: 48% reduction in CP per ovule with a 100-fold increase in floral abundance), as hypothesized (Fig. 1e, Table 1, H2.2). In contrast to the numeric assurance hypothesis (Fig. 1, Table 1, H4), abundance did not directly enhance joint fitness gain but in fact showed a weak negative effect ($r = -0.08$) (Fig. 2a). Overall, the results suggest that rarer species experience a slight increase in receipt of HP but benefit from more CP from the co-transport of HP–CP, whereas more abundant species experience greater misplacement of CP and do not automatically have higher joint fitness gain via numeric assurance.

Our findings support the hypothesis that plant–pollinator interactions favour rare species in species-rich co-flowering communities, and this has the potential to contribute to the maintenance of flowering plant diversity. Specifically, we showed that the net effects of generalization and abundance cause appreciable reduction in CP per ovule, which may affect seed quantity or quality (Supplementary Notes). To our knowledge, no other study to date has contrasted multiple pollination-mediated mechanisms of diversity maintenance. Here pollinator niche partitioning that leads to non-nestedness and modularity is essential for coexistence between rare and abundant species in this co-flowering community, where temporal niche partitioning is limited by rapid seasonal drying (Methods). When plants do share some pollinator resources, asymmetric facilitation can serve as an alternative diversity-promoting mechanism, as seen in diverse highlands and semi-desert plant communities^{17,22}. By contrast, the presumed benefits of numeric abundance and self-pollination were not well supported in this community. The lack of numeric assurance may point to the complexity in spatial distributions of diverse co-flowering plant species, which rarely fit the situations that promote numeric advantage (randomly distributed or monocultures^{26,34}) but rather intermingle within the community, promoting pollinator visits among species and facilitation³⁴. The lack of pollination assurance in this community may reflect the fact that rarer species had lower abilities for autonomous self-pollination than more abundant species, and thus they required, and benefitted from, pollinator-mediated processes described above. Whether the relative strengths of these mechanisms are universal awaits

further community-level studies. Our findings are probably relevant in species-rich communities or communities of low phenotypic complementarity or environmental seasonality where the nestedness of plant–pollinator interactions is probably low^{35,36}.

Our results demonstrate the importance of considering community-wide interactions between plants and pollinators that affect fertilization success^{13,17}, which set the stage for mechanisms that operate at later life stages (for example, seedling survival and growth) to ultimately contribute to the population dynamics of coexisting plant species. We note that a full understanding of diversity-promoting mechanisms during plant reproduction requires further exploration of whether reproduction is limited most by pollination processes documented here or by ovule or resource availability. Nevertheless, considering pollination in the maintenance of plant diversity has immediate application for conservation as it indicates that functioning communities of plants and pollinators—not just plant species—need to be conserved. These considerations are more urgent than ever for conservation of biodiversity as changes in plant–pollinator mutualisms are becoming commonplace⁶. In light of pollinator losses worldwide⁷, overall diminished pollinator niche space may intensify plant competition and do so at the detriment of rare species that are more specialized than abundant species. Furthermore, climatically induced shifts in plant abundance³⁷ may alter community-wide floral trait variation that is key to pollinator niche partitioning and subsequent pollen transport dynamics, and may also affect the strength of asymmetric facilitation if rare and abundant species respond differently to climate change. Thus, our results argue for a refocusing on the importance of plant–pollinator interactions for the persistence of rare species and biodiversity conservation in the rapidly changing communities of the Anthropocene³⁸.

Online content

Any methods, additional references, Nature Research reporting summaries, source data, extended data, supplementary information, acknowledgements, peer review information; details of author contributions and competing interests; and statements of data and code availability are available at <https://doi.org/10.1038/s41586-021-03890-9>.

1. Hubbell, S. P. *The Unified Neutral Theory of Biodiversity and Biogeography* (Princeton Univ. Press, 2001).
2. Wills, C. et al. Nonrandom processes maintain diversity in tropical forests. *Science* **311**, 527–531 (2006).
3. Chesson, P. Mechanisms of maintenance of species diversity. *Annu. Rev. Ecol. Evol. Syst.* **31**, 343–366 (2000).
4. Ollerton, J. Pollinator diversity: distribution, ecological function, and conservation. *Annu. Rev. Ecol. Evol. Syst.* **48**, 353–376 (2017).
5. Vamosi, J. C. et al. Pollination decays in biodiversity hotspots. *Proc. Natl Acad. Sci. USA* **103**, 956–961 (2006).
6. Bennett, J. M. et al. Land use and pollinator dependency drives global patterns of pollen limitation in the Anthropocene. *Nat. Commun.* **11**, 3999 (2020).
7. Potts, S. G. et al. Global pollinator declines: trends, impacts and drivers. *Trends Ecol. Evol.* **25**, 345–353 (2010).
8. Vamosi, J. C., Magallon, S., Mayrose, I., Otto, S. P. & Sauquet, H. Macroevolutionary patterns of flowering plant speciation and extinction. *Annu. Rev. Plant Biol.* **69**, 685–706 (2018).

9. Ollerton, J., Winfree, R. & Tarrant, S. How many flowering plants are pollinated by animals? *Oikos* **120**, 321–326 (2011).
10. Rodger, J. G. et al. 2021 Widespread vulnerability of plant seed production to pollinator decline. *Sci. Adv.* (in the press).
11. Pimm, S. L., Jones, H. L. & Diamond, J. On the risk of extinction. *Am. Nat.* **132**, 757–785 (1988).
12. Sargent, R. D. & Ackerly, D. D. Plant–pollinator interactions and the assembly of plant communities. *Trends Ecol. Evol.* **23**, 123–130 (2008).
13. Benadi, G. & Pauw, A. Frequency dependence of pollinator visitation rates suggests that pollination niches can allow plant species coexistence. *J. Ecol.* **106**, 1892–1901 (2018).
14. Bruno, J. F., Stachowicz, J. J. & Bertness, M. D. Inclusion of facilitation into ecological theory. *Trends Ecol. Evol.* **18**, 119–125 (2003).
15. Benadi, G., Bluthgen, N., Hovestadt, T. & Poethke, H. J. Population dynamics of plant and pollinator communities: stability reconsidered. *Am. Nat.* **179**, 157–168 (2012).
16. Moeller, D. A. Facilitative interactions among plants via shared pollinators. *Ecology* **85**, 3289–3301 (2004).
17. Bergamo, P. J., Susin Streher, N., Traveset, A., Wolowski, M. & Sazima, M. Pollination outcomes reveal negative density-dependence coupled with interspecific facilitation among plants. *Ecol. Lett.* **23**, 129–139 (2020).
18. Barrett, S. C. H. The evolution of plant sexual diversity. *Nat. Rev. Genet.* **3**, 274–284 (2002).
19. Ashman, T. L. & Arceo-Gómez, G. Toward a predictive understanding of the fitness costs of heterospecific pollen receipt and its importance in co-flowering communities. *Am. J. Bot.* **100**, 1061–1070 (2013).
20. Moreira-Hernández, J. I. & Muchhala, N. Importance of pollinator-mediated interspecific pollen transfer for angiosperm evolution. *Annu. Rev. Ecol. Evol. Syst.* **50**, 191–217 (2019).
21. Ashman, T. L. et al. Pollen limitation of plant reproduction: ecological and evolutionary causes and consequences. *Ecology* **85**, 2408–2421 (2004).
22. Tur, C., Saez, A., Traveset, A. & Aizen, M. A. Evaluating the effects of pollinator-mediated interactions using pollen transfer networks: evidence of widespread facilitation in south Andean plant communities. *Ecol. Lett.* **19**, 576–586 (2016).
23. Levin, D. A. & Anderson, W. W. Competition for pollinators between simultaneously flowering species. *Am. Nat.* **104**, 455–467 (1970).
24. Ashman, T. L., Alonso, C., Parra-Tabla, V. & Arceo-Gómez, G. Pollen on stigmas as proxies of pollinator competition and facilitation: complexities, caveats and future directions. *Ann. Bot.* **125**, 1003–1012 (2020).
25. Lloyd, D. G. Some reproductive factors affecting the selection of self-fertilization in plants. *Am. Nat.* **113**, 67–79 (1979).
26. Sargent, R. D. & Otto, S. P. The role of local species abundance in the evolution of pollinator attraction in flowering plants. *Am. Nat.* **167**, 67–80 (2006).
27. Adler, P. B., Fajardo, A., Kleinhesselink, A. R. & Kraft, N. J. B. Trait-based tests of coexistence mechanisms. *Ecol. Lett.* **16**, 1294–1306 (2013).
28. Armbruster, W. S. The specialization continuum in pollination systems: diversity of concepts and implications for ecology, evolution and conservation. *Funct. Ecol.* **31**, 88–100 (2017).
29. Minnaar, C., Anderson, B., de Jager, M. L. & Karron, J. D. Plant–pollinator interactions along the pathway to paternity. *Ann. Bot.* **123**, 225–245 (2019).
30. Kantsa, A. et al. Disentangling the role of floral sensory stimuli in pollination networks. *Nat. Commun.* **9**, 1041 (2018).
31. Fang, Q. & Huang, S. Q. A directed network analysis of heterospecific pollen transfer in a biodiverse community. *Ecology* **94**, 1176–1185 (2013).
32. Baldwin, B. G. Origins of plant diversity in the California floristic province. *Annu. Rev. Ecol. Evol. Syst.* **45**, 347–369 (2014).
33. Bascompte, J., Jordano, P., Melian, C. J. & Olesen, J. M. The nested assembly of plant–animal mutualistic networks. *Proc. Natl Acad. Sci. USA* **100**, 9383–9387 (2003).
34. Thomson, J. D., Fung, H. F. & Ogilvie, J. E. Effects of spatial patterning of co-flowering plant species on pollination quantity and purity. *Ann. Bot.* **123**, 303–310 (2019).
35. Rezende, E. L., Lavabre, J. E., Guimaraes, P. R., Jordano, P. & Bascompte, J. Non-random coextinctions in phylogenetically structured mutualistic networks. *Nature* **448**, 925–928 (2007).
36. Song, C. L., Rohr, R. P. & Saavedra, S. Why are some plant–pollinator networks more nested than others? *J. Anim. Ecol.* **86**, 1417–1424 (2017).
37. Hegland, S. J., Nielsen, A., Lazaro, A., Bjerknes, A. L. & Totland, O. How does climate warming affect plant–pollinator interactions? *Ecol. Lett.* **12**, 184–195 (2009).
38. Ohlemuller, R. et al. The coincidence of climatic and species rarity: high risk to small-range species from climate change. *Biol. Lett.* **4**, 568–572 (2008).

Publisher's note Springer Nature remains neutral with regard to jurisdictional claims in published maps and institutional affiliations.

© The Author(s), under exclusive licence to Springer Nature Limited 2021

Methods

Study site and co-flowering community

The co-flowering community of the species-rich serpentine seep system at the McLaughlin Natural Reserve in California, USA (38.8582° N, 122.4093° W) is the subject of this study. The unique soil chemistry of these serpentine seeps (small ephemeral streams) and late summer moisture are important determinants of species that can survive in this grassland/scrub environment. Many of these small herbaceous annuals and perennials³⁹ are serpentine endemics (approximately 20%), which are regionally rare species. In this system, pollination is a strong force acting on successful reproduction and probably coexistence, because seep drying restricts flowering and fruiting time, enforcing substantial flowering overlap and pollinator-mediated plant–plant interactions^{39–41}. As a result, temporal niche partitioning among plant species is limited in terms of pollinator resources. We focused on a system that consisted of five seeps (Extended Data Table 1), separated by 0.3–5 km (ref.⁴⁰). Each seep was visited once every week during the peak of flowering season (April–June) for a total of 9–10 weeks per year in 2016 and 2017. Despite some differences in flowering phenology (Supplementary Table 3), our study captured the major flowering periods across the herbaceous, non-graminoid species, as flowering generally tapers off after the end of June for the majority of species in these seeps³⁹.

Plant–pollinator interactions

Each week, plants at each seep were scored for plant–pollinator interactions. Observations were conducted between 0800 and 1700 hours by two to three people simultaneously. For the two species with crepuscular flowers (*Linanthus dichotomus* and *Chlorogalum pomeridianum*), pollinator observations were extended to 19:00 hours. All pollinators visiting a plant species were collected with a sweep net for identification with the exception of hummingbirds. We considered a legitimate plant–pollinator interaction only when a pollinator contacted the reproductive parts of a flower, although we note that this interaction alone does not confirm that a given visitor has a positive effect on pollination and/or reproductive success. Lepidopteran insects were preserved dry, and non-lepidopteran insects were preserved with 100% ethanol in 1.5-ml microcentrifuge tubes in a –20 °C freezer until processed and pinned. Pinned or ethanol-preserved specimens were identified by experts to the lowest taxonomic level possible (typically species level; Supplementary Methods). Vouchered specimens were deposited at the Carnegie Museum of Natural History (Pittsburgh, PA, USA).

As we aimed to collect an equal number of pollinators per plant species ($n = 150$ on average) evenly across seeps and years, each plant species was observed for 20–30 min per day. More time was invested (1–2 h per day) observing plants that were infrequently visited. Despite additional time invested, it did not yield more pollinator observations for some species, including the species that flowered in the evening (for example, *L. dichotomus*) or had exceptionally small flowers (for example, *Hesperolin californicum*, *Heterocodon rariflorus* and *Githopsis specularioides*). Rarefaction analysis (Extended Data Fig. 2) using the package iNEXT⁴² in R v.3.6.0⁴³ showed that our sampling effort captured the majority of pollinator diversity for each of the 79 plant species (Extended Data Fig. 2a, b), especially for the plant species ($n = 64$; Extended Data Fig. 2c, d) that were included in the downstream PSEMs.

Style collection

To characterize interspecific pollen transfer, styles from spent flowers of each species were collected on the same day as pollinator observations. Styles were collected from different individuals of each species in all cases except the very rare species. Three styles per species were stored together in a 1.5-ml microcentrifuge tube with 70% ethanol. For species with flowers that were too small to remove styles in the field ($n = 9$), we collected and stored whole flowers, and then styles were

taken from these flowers in the laboratory with the aid of a dissecting microscope. From this vast collection of styles, we used a stratified random subsampling across all seeps and both years to achieve 90 (18 × 5) date–seep combinations, and a total of 54 styles per species for stigma pollen identification following the recommendation⁴⁴. Fourteen species (Supplementary Methods) were below our sampling goal (at least 36 styles per species; mean = 54 styles) and were excluded from downstream interspecific pollen transfer network and PSEMs.

Abundance/rarity

Floral abundances were determined from weekly surveys of fixed plots (1 m × 3 m each) at each seep in both years (Extended Data Table 1). Plots were positioned along the length of each seep 1–20 m apart to capture plant species diversity within a site. At each sampling date, we recorded all open flowers for each species within a plot. For Asteraceae, we counted compact ‘heads’ as individual floral units. These surveys were carried out primarily during 12:30–14:00 hours and were extended to 19:00 hours for species with crepuscular flowers. Floral abundance of each species was summed across fixed plots, seeps and years for downstream PSEMs. Here species rarity based on floral abundance was correlated with species occurrence (in the number of surveyed plots, two-sided Pearson’s correlation test, $r = 0.64$, $t = 6.9$, d.f. = 70, $P = 1.8 \times 10^{-9}$; Extended Data Fig. 3b).

Floral traits

Flowers were collected from separate individuals of each species across one or more seeps, depending on rarity and stored in 70% ethanol. For 10 flowers per species, we measured 20 floral traits and subsequently categorized them according to their functions: attraction traits ($n = 7$), male ($n = 8$) and female ($n = 5$) organ traits (Extended Data Figs. 4–6). Three (*Adenostoma fasciculatum*, *Collomia diversifolia* and *Hoita macrostachya*) of the 72 species that were measured for floral traits (Supplementary Table 3) had no pollinator observations and were excluded from additional analyses.

The attraction traits included flower colour, shape, symmetry, restrictiveness, inflorescence type, flower tube length and corolla limb length. Male organ traits included anther length, stamen number, height and exertion, and pollen shape, texture, area and width-to-length ratio. Female organ traits included style length, stigma–anther distance, and stigma shape, area and exposure. The definitions and measurements of individual traits are described in Supplementary Methods.

Pollen identification on stigmas

To taxonomically identify pollen grains on stigmas, we created a pollen library for all flowering plant species in the seeps⁴⁵ (R.A.H., N. Cullen, R.L.K. and T.-L.A., in review). Species-specific pollen traits (that is, size, shape, texture and aperture numbers) were obtained for acetolysed pollen collected from anthers of flowers in the seeps. Flowers from non-focal plants outside the seeps (for example, grasses and trees) were also collected to facilitate the identification of pollen communities received by individual stigmas.

To characterize CP and HP received by stigmas, we acetolysed⁴⁶ on average 54 styles (range = 36–57) from each species sampled in a stratified random manner across all seeps and years, as described above (see ‘Style collection’). Specifically, we acetolysed the contents of each sample tube (three styles and their pollen grains) to achieve a volume of 20 μ l. We then enumerated pollen of a 5 μ l aliquot using a haemocytometer and calculated the total amount of pollen grains per style. When pollen was too dense to count, we diluted the 20 μ l to 100 or 200 μ l and adjusted final counts accordingly. Each pollen grain was identified to species (including both CP and HP) on the basis of the pollen library. When pollen was from species not present in the pollen library, we designated it as from a specific unknown species (for example, U1, U2, and so on). However, in cases in which we were unable to distinguish a pollen grain among congeners or morphologically similar species,

we assigned it to a congener or morphospecies group. We then used a fractional identity approach to assign pollen grains within these groups. Fractional identity was based on relative probabilities as a function of floral abundance at the sampling seep and date. To examine how fractional identity influenced the estimate of HP on stigmas, we compared the richness of HP when fractional identities were excluded and included. A strong positive relationship between the two approaches was observed (general linear model, slope = 0.73, $t = 17.1$, $P < 2 \times 10^{-16}$; Extended Data Fig. 8a), supporting the use of fractional identity. Rarefaction analysis of pollen grains (with fractional identity) showed that our sampling effort of styles captured the majority of HP donor species for each recipient species (Extended Data Fig. 8b, c).

To account for variation in the number of sampled styles among species, we standardized pollen data to the same number of styles ($n = 54$) across species, which outperforms standardization based on rarefaction in preventing information loss and detecting differences among samples (that is, pollen loads of individual species on stigmas)⁴⁷. The standardized pollen data (Supplementary Table 5) were used for the interspecific pollen transfer network.

Plant phylogeny

The phylogenetic tree of all 79 co-flowering species was constructed on the basis of PhytoPhylo megaphylogeny of vascular plants^{48,49} and the Open Tree of Life⁵⁰ using the R packages *ape*⁵¹, *rotl*⁵² and *phytools*⁵³, as described in Supplementary Methods.

Multivariate analyses of floral traits

To examine floral trait variation among co-flowering species, we used the trait mean averaged across the 10 flowers of each species. We first assessed the overall floral trait variation by performing a factor analysis of mixed data (FAMD) of all the 20 quantitative and qualitative traits using the package *FactoMineR*⁵⁴ (Extended Data Fig. 3a). Instead of imputation, missing data were omitted from the FAMD. We then performed FAMD for attraction, male and female organ traits independently, and used the first three dimensions from each for subsequent PSEMs. Our choice of the first three dimensions aimed to capture a large amount of trait variation (48–71% here) while avoiding overparameterizing PSEMs. It is worth noting that different from multivariate analyses of quantitative data (for example, principal component analysis), in FAMD, the same qualitative trait can contribute to more than one independent FAMD dimension, because of multiple (more than two, not binary) categories within each qualitative trait.

Plant–pollinator network

We constructed the network based on 7,324 total plant–pollinator interactions observed across all seeps in both years using the package *bipartite*⁵⁵. To evaluate pollinator niche partitioning, we assessed whether co-flowering plant species were limited in pollinator sharing, that is, more specialized than expected by random interactions with pollinator partners, at the species, group (of plants as a whole) and network levels using multiple metrics. At the species level, we used the metrics of (1) pollinator Shannon diversity, which considers both pollinator richness and interaction frequencies, and (2) similarity between pollinator use and availability (that is, proportional similarity)⁵⁶, which indicates increased generalization when it increases from 0 to 1. At the group level, we used the metrics of (3) mean number of shared pollinator partners between any two plants, and (4) mean similarity in pollinator assemblage between any two plants (that is, niche overlap using Horn's index in *bipartite*)⁵⁷, which considers both pollinator identity and interaction frequencies. At the network level, we used (5) NODF (nestedness overlap and decreasing fill)⁵⁸ and (6) its weighted version that takes into account interaction frequencies in *bipartite*, and (7) modularity in package *igraph*⁵⁹. Unweighted and weighted NODF reflect specialization asymmetry (that is, specialist plants interacting with the subset of pollinator partners of generalist plants), with

increased nestedness when the metrics increase from 0 to 100. To estimate modularity, we converted the two-mode plant–pollinator network into one-mode network using *bipartite*, and then estimated modularity based on the fast greedy modularity optimization algorithm implemented in *igraph*. For the next step, we compared these observed metrics to null models. We constructed the null model by rewiring interactions while keeping total interaction frequencies of individual plants and pollinators constant (that is, the *r2dtable* algorithm)⁶⁰ using the packages *bipartite* and *vegan*⁶¹. For modularity, the '*r2dtable*' null model was converted to one mode as described above. On the basis of 1,000 random replications of the null model, we obtained null distributions of individual metrics, and calculated the null mean and the 95% confidence intervals (that is, the 2.5th and 97.5th percentiles). The statistical significance of each observed metric was obtained by comparing the observed value to the null confidence intervals. The two-sided P value was calculated as how often the observed metric was greater or smaller than all 1,000 random replicates.

The plant–pollinator network was visualized as an interaction matrix (Extended Data Fig. 1) using the package *ggplot2*⁶². Plant species were arranged according to their phylogenetic positions. Pollinator species were arranged according to the number and community assemblage of the plant species that they visited, the latter of which was obtained using the first axis of a canonical correspondence analysis in the package *vegan*.

Interspecific pollen transfer network and pollination-mediated fitness

A pollen transfer network that describes pollinator-mediated pollen delivery among co-flowering plants was constructed using the package *igraph*⁵⁹, on the basis of pollen data standardized to the same number of styles per species ($n = 54$) and using fractional identity as described above (see 'Pollen identification on stigmas'; Supplementary Table 5). The standardized pollen receipt can remove variation in sampling effort and effectively reflect per capita estimates of pollen received and donated for each species. In this directed pollen transfer network (Extended Data Fig. 7), visualized using *Gephi* v0.9.2⁶³, the arrows link pollen donor to recipient species. For a focal species, the number of incoming arrows represents the number of heterospecific plant species from which the focal plant species receives pollen. The arrow widths represent the amount of pollen from individual donors, the sum of which ('strength-in' in *igraph*) indicates total receipt of HP for that plant species. By contrast, outgoing arrows indicate the number of heterospecific species to which a focal species donates pollen, and the total amount ('strength-out') indicates its CP that is misdelivered to coexisting heterospecific plants (that is, misplacement of CP). These estimates of species-level pollinator-mediated receipt of HP and misplacement of CP were used in the PSEMs described below.

The successful pollination outcome of pollen transport is deposition of CP on conspecific stigmas

This is a per capita estimate of joint (male and female) fitness gain as it represents their mating success (via male and female gametes), based on the standardized pollen receipt data. We normalized this estimate of joint fitness gain by accounting for the differences across species in female gametes (that is, ovule number), as CP per ovule. Ovule number was obtained from field-collected, ethanol-preserved flowers that were collected for floral trait measurements (see 'Floral traits') or from our previous greenhouse studies (*Diplacus layneae*, *Erythranthe guttata* and *Erythranthe nudata*)⁶⁴.

Phylogenetic signal

To test for evolutionary dependence among co-flowering species, we first examined the phylogenetic signals of floral traits (20 traits as well as the first three FAMD dimensions of attraction, male and female organ traits separately), pollinator niche breadth (species-level metrics

from the plant–pollinator network) and pollination-mediated fitness estimates (receipt of HP, misplacement of CP and CP per ovule), using the packages *phylosignal*⁶⁵ and *caper*⁶⁶ (Supplementary Methods). In contrast to pollinator niche breadth and pollination-mediated fitness, floral traits including FAMD dimensions exhibited strong phylogenetic signals (Supplementary Table 4). Such evolutionary dependence was considered in subsequent PSEMs.

PSEMs

We conducted PSEMs to link floral traits and plant rarity (abundance) to pollination niche breadth (generalization) and pollination-mediated fitness losses and gains, and thereby we could test explicitly the paths associated with pollinator niche partitioning, asymmetric facilitation and automatic assurances (pollination assurance and numeric assurance) (Fig. 1, Table 1). This resulted in a complete dataset on 64 plant species for the PSEMs. Specifically, we built four nested models (Extended Data Fig. 9). Model 1 described pollinator niche partitioning and asymmetric facilitation. Relative to model 1, model 2 added the hypothesis of pollination assurance via autonomous self-pollination in light of numeric assurance of abundance²⁶ (collectively referred to as automatic assurances), whereas model 3 added pollination assurance alone and model 4 added numeric assurance alone.

In model 1, the joint fitness gain (CP per ovule) was hypothesized to be influenced by pollinator niche (generalization) and pollinator-mediated receipt of HP (Extended Data Fig. 9a) and misplacement of CP (Extended Data Fig. 9b). In models 2–4 (Extended Data Fig. 9c–h), the joint fitness gain was hypothesized to be directly influenced by a trait that affects the potential for self-pollen deposition (stigma–anther distance)⁶⁷ and/or abundance as well, to test for the influence of pollination and/or numeric assurance. In all models, to assess the floral traits that govern pollinator niche (generalization), we tested the roles of attraction traits and male organ traits that potentially signal pollen reward. We found that male organ traits either resulted in a poor model fit or did not improve a model fit in PSEMs. Thus, we only considered attraction traits influencing pollinator niche (Extended Data Fig. 9). Pollinator-mediated receipt of HP was hypothesized to be influenced by female organ traits, whereas misplacement of CP was hypothesized to be influenced by male organ traits (Extended Data Fig. 9). In these models, the positive unidirectional (rather than bidirectional) arrow from abundance to generalization reflected that generalization is not a sufficient condition for abundance⁶⁸, due to processes that operate at the pollination stage (for example, potential fitness costs of generalization, this study) and at later life stages (for example, seedling survival and growth).

The PSEMs comprised PGLSs (using the *gls* function with Pagel's algorithm in the package *nlme*⁶⁹) to account for evolutionary dependence among species and were fitted using the package *piecewiseSEM*⁷⁰. To improve normality in PSEMs, we power transformed the variables when necessary, with the optimal power parameter determined using the Box–Cox method in the package *car*⁷¹ before PGLSs. Specifically, natural logarithm transformation was applied to floral abundance, CP per ovule and receipt of HP, and the optimal power parameter was 0.2 for misplacement of CP. For pollination generalization at the species level, we used pollinator Shannon diversity as described above, because this metric considered both pollinator richness and interaction frequencies and showed a strong correlation with the other species-level metric (that is, similarity between pollinator use and availability; two-sided Pearson's correlation test, $r = 0.79$, $t = 11.3$, d.f. = 77, $P < 2.2 \times 10^{-16}$), with the least assumptions relative to derived metrics⁷². The estimate of pollinator Shannon diversity based on the original data of plant–pollinator interactions was used, as it was consistent with the estimate based on the standardized data (to the median pollinator observations across species; two-sided Pearson's correlation test, $r = 1$, $t = 97.4$, d.f. = 77, $P < 2.2 \times 10^{-16}$). For stigma–anther distance, we used the fourth dimension (Dim 4) of female function traits (Extended Data Fig. 6) instead of the raw data to ensure the absence of collinearity

among predictors in PGLSs, which was confirmed using variance inflation factors in the package *car*⁷¹. The goodness-of-fit of each PSEM was evaluated using two-sided Fisher's *C* statistic based on Shipley's d-separation (directed separation) test of conditional independencies⁷³. Good model fits were confirmed in all the PSEMs ($P > 0.05$ for Fisher's *C* statistic; Extended Data Fig. 9). Nested model comparisons in *piecewiseSEM* used Akaike's information criterion (AIC)⁷³.

We further fitted the same set of PSEMs using the package *phylopath*⁷⁴ that is also based on Shipley's d-separation, to ensure the robustness of the estimation of standardized coefficients (r) and to facilitate model averaging when more than one competing model was supported. Different from *piecewiseSEM*, the 95% confidence intervals of individual standardized coefficients were obtained via bootstrapping ($n = 1,000$) in *phylopath*. Nested model comparisons in *phylopath* used the *C* statistic information criterion corrected for small sample sizes (CICc)⁷⁴.

Following recommendations^{73,74}, the best-supported model produces the lowest AIC or the lowest CICc, whereas models are rejected with greater than 3 units difference from the best model (Δ AIC or Δ CICc). For models assessing mechanisms via receipt of HP, model 1 and model 4 were consistently identified as the supported models in both *piecewiseSEM* and *phylopath* (Extended Data Fig. 9), and thus model averaging was performed using *phylopath* in which the path coefficients were averaged across the supported models while taking into account the CICc weights of each model⁷⁴, and presented in Fig. 2a. For models assessing mechanisms via misplacement of CP, model 1 was consistently identified as the best-supported model (Extended Data Fig. 9), and reported in Fig. 2b (*phylopath*) and Supplementary Table 6 (*piecewiseSEM*).

On the basis of the model-averaged or single path diagram after model selection, the strength and sign of individual paths for hypotheses were calculated as the product of the standardized coefficients.

Reporting summary

Further information on research design is available in the Nature Research Reporting Summary linked to this paper.

Data availability

All data that support the findings of this study are included in this published article and its Supplementary Information files and source data files. Source data are provided with this paper.

Code availability

All software used in this study are provided in the Methods, Supplementary Information and the accompanying Reporting Summary.

39. Arceo-Gómez, G., Kaczorowski, R. L. & Ashman, T.-L. A network approach to understanding patterns of coflowering in diverse communities. *Int. J. Plant Sci.* **179**, 569–582 (2018).
40. Koski, M. H. et al. Plant–flower visitor networks in a serpentine metacommunity: assessing traits associated with keystone plant species. *Arthropod Plant Interact.* **9**, 9–21 (2015).
41. Arceo-Gómez, G. et al. Patterns of among- and within-species variation in heterospecific pollen receipt: the importance of ecological generalization. *Am. J. Bot.* **103**, 396–407 (2016).
42. Chao, A. et al. Rarefaction and extrapolation with Hill numbers: a framework for sampling and estimation in species diversity studies. *Ecol. Monogr.* **84**, 45–67 (2014).
43. R Core Team. *R: A Language and Environment for Statistical Computing*, <https://www.R-project.org/> (R Foundation for Statistical Computing, 2019).
44. Arceo-Gómez, G., Alonso, C., Ashman, T.-L. & Parra-Tabla, V. Variation in sampling effort affects the observed richness of plant–plant interactions via heterospecific pollen transfer: implications for interpretation of pollen transfer networks. *Am. J. Bot.* **105**, 1601–1608 (2018).
45. Hayes, R. A., Cullen N., Kaczorowski R. L., O'Neill E. M. & Ashman T.-L. A community-wide description and key of pollen from co-flowering plants of the serpentine seeps of McLaughlin Reserve. *Madrone* (in the press).
46. Dafni, A. *Pollination Ecology: a Practical Approach* (Oxford Univ. Press, 1992).
47. McMurdie, P. J. & Holmes, S. Waste NOT, want not: why rarefying microbiome data is inadmissible. *PLoS Comp. Biol.* **10**, e1003531 (2014).

48. Qian, H. & Jin, Y. An updated megaphylogeny of plants, a tool for generating plant phylogenies and an analysis of phylogenetic community structure. *J. Plant Ecol.* **9**, 233–239 (2016).
49. Zanne, A. E. et al. Three keys to the radiation of angiosperms into freezing environments. *Nature* **506**, 89–92 (2014).
50. Hinchliff, C. E. et al. Synthesis of phylogeny and taxonomy into a comprehensive tree of life. *Proc. Natl Acad. Sci. USA* **112**, 12764–12769 (2015).
51. Paradis, E. & Schliep, K. ape 5.0: an environment for modern phylogenetics and evolutionary analyses in R. *Bioinformatics* **35**, 526–528 (2019).
52. Michonneau, F., Brown, J. W. & Winter, D. J. rotl: an R package to interact with the Open Tree of Life data. *Methods Ecol. Evol.* **7**, 1476–1481 (2016).
53. Revell, L. J. phytools: an R package for phylogenetic comparative biology (and other things). *Methods Ecol. Evol.* **3**, 217–223 (2012).
54. Le, S., Josse, J. & Husson, F. FactoMineR: an R package for multivariate analysis. *J. Stat. Softw.* **25**, 1–18 (2008).
55. Dormann, C. F., Gruber, B. & Fruend, J. Introducing the bipartite package: analysing ecological networks. *R News* **8**, 8–11 (2008).
56. Feinsinger, P., Spears, E. E. & Poole, R. W. A simple measure of niche breadth. *Ecology* **62**, 27–32 (1981).
57. Horn, H. S. Measurement of "overlap" in comparative ecological studies. *Am. Nat.* **100**, 419–424 (1966).
58. Almeida-Neto, M., Guimaraes, P., Guimaraes, P. R., Loyola, R. D. & Ulrich, W. A consistent metric for nestedness analysis in ecological systems: reconciling concept and measurement. *Oikos* **117**, 1227–1239 (2008).
59. Csardi, G. & Nepusz, T. The igraph software package for complex network research. *InterJournal* **1695**, 1–9 (2006).
60. Patefield, W. Algorithm AS 159: an efficient method of generating random $R \times C$ tables with given row and column totals. *Appl. Stat.* **30**, 91–97 (1981).
61. Oksanen, J. et al. vegan: Community Ecology Package. R package version 2.5–5, <https://CRAN.R-project.org/package=vegan> (2019).
62. Wickham, H. *ggplot2: Elegant Graphics for Data Analysis* (Springer, 2016).
63. Bastian, M., Heymann, S. & Jacomy, M. Gephi: an open source software for exploring and manipulating networks. Presented at the Third international AAAI Conference on Weblogs and Social Media (2009).
64. Arceo-Gómez, G., Kaczorowski, R. L., Patel, C. & Ashman, T. L. Interactive effects between donor and recipient species mediate fitness costs of heterospecific pollen receipt in a co-flowering community. *Oecologia* **189**, 1041–1047 (2019).
65. Keck, F., Rimet, F., Bouchez, A. & Franc, A. phyllosignal: an R package to measure, test, and explore the phylogenetic signal. *Ecol. Evol.* **6**, 2774–2780 (2016).
66. Orme, D. et al. caper: comparative analyses of phylogenetics and evolution in R. R package version 1.0.1, <https://CRAN.R-project.org/package=caper> (2018).
67. Barrett, S. C. H. The evolution of plant sexual diversity. *Nat. Rev. Genet.* **3**, 274–284 (2002).
68. Fort, H., Vazquez, D. P. & Lan, B. L. Abundance and generalisation in mutualistic networks: solving the chicken-and-egg dilemma. *Ecol. Lett.* **19**, 4–11 (2016).
69. Pinheiro, J., Bates, D., DebRoy, S., Sarkar, D. & R Core Team. nlme: linear and nonlinear mixed effects models. R package version 3.1-143, <https://CRAN.R-project.org/package=nlme> (2019).
70. Lefcheck, J. S. & Freckleton, R. piecewiseSEM: piecewise structural equation modelling in R for ecology, evolution, and systematics. *Methods Ecol. Evol.* **7**, 573–579 (2015).
71. Fox, J. & Weisberg, S. *An R companion to Applied Regression*, 3rd edition (Sage, 2019).
72. Blüthgen, N., Menzel, F. & Blüthgen, N. Measuring specialization in species interaction networks. *BMC Ecol.* **6**, 9 (2006).
73. Shipley, B. The AIC model selection method applied to path analytic models compared using a d-separation test. *Ecology* **94**, 560–564 (2013).
74. van der Bijl, W. phylopath: easy phylogenetic path analysis in R. *PeerJ* **6**, e4718 (2018).

Acknowledgements We thank J. Baker, D. Chang, A. M. Arters, U. Meenakshinathan, K. Doleski, S. Barratt-Boyes, R. A. Ashman and M. Holden for assistance with stigma pollen identification, floral trait measurements and insect specimen processing; J. Rawlins, J. Pawelek, R. Androw and B. Coulter for insect identification; J. Hyland and V. Verdecia for logistic support at the Carnegie Museum of Natural History; McLaughlin field station staff for logistical support of field work; and the members of the Ashman, Wood and Turcotte laboratories for discussion. This work was supported by the National Science Foundation (DEB 1452386) to T.-L.A.

Author contributions T.-L.A. conceived the study. N.W. and T.-L.A. led the conceptual development. N.W. analysed the data. N.W., T.-L.A. and R.L.K. wrote the manuscript. N.W., T.-L.A., R.L.K. and G.A.-G. contributed to manuscript revisions. R.L.K., E.M.O., R.A.H., G.A.-G. and T.-L.A. collected the data.

Competing interests The authors declare no competing interests.

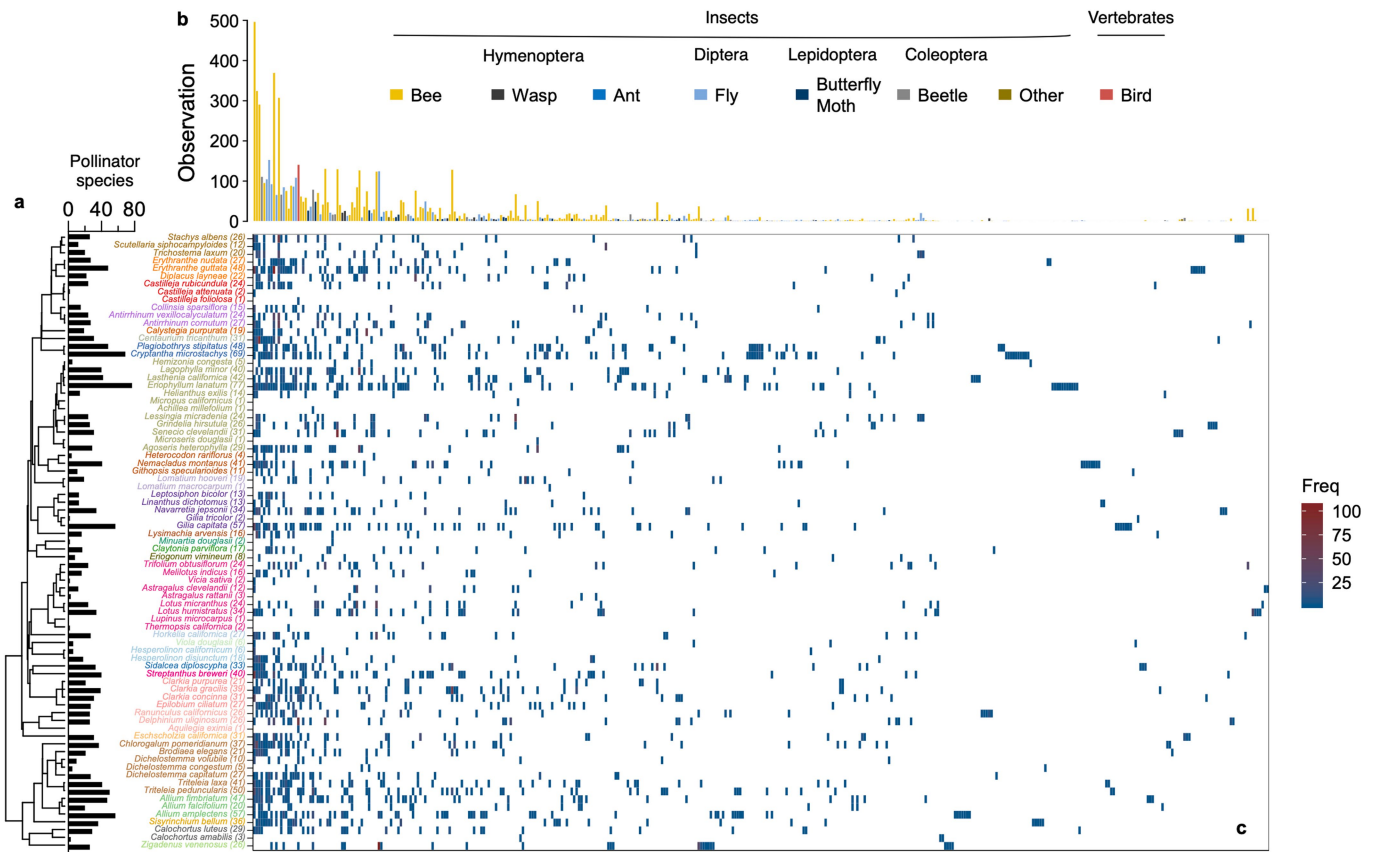
Additional information

Supplementary information The online version contains supplementary material available at <https://doi.org/10.1038/s41586-021-03890-9>.

Correspondence and requests for materials should be addressed to N.W. or T.-L.A.

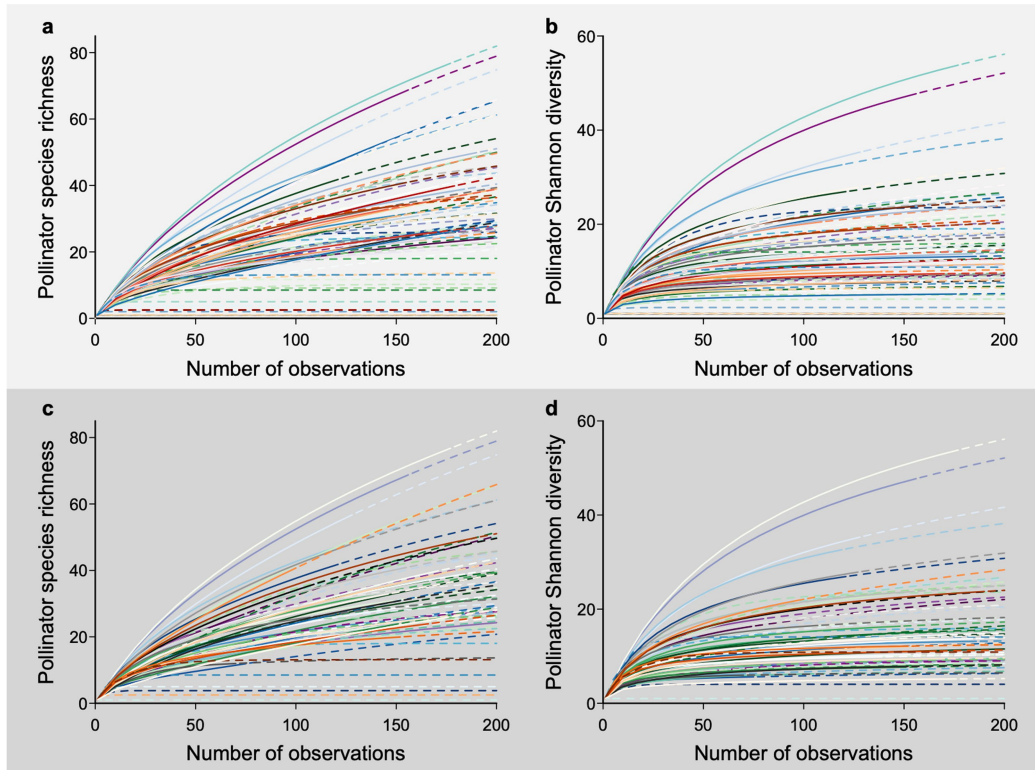
Peer review information *Nature* thanks Marcelo Aizen, Christopher Kaiser-Bunbury and the other, anonymous, reviewer(s) for their contribution to the peer review of this work.

Reprints and permissions information is available at <http://www.nature.com/reprints>.



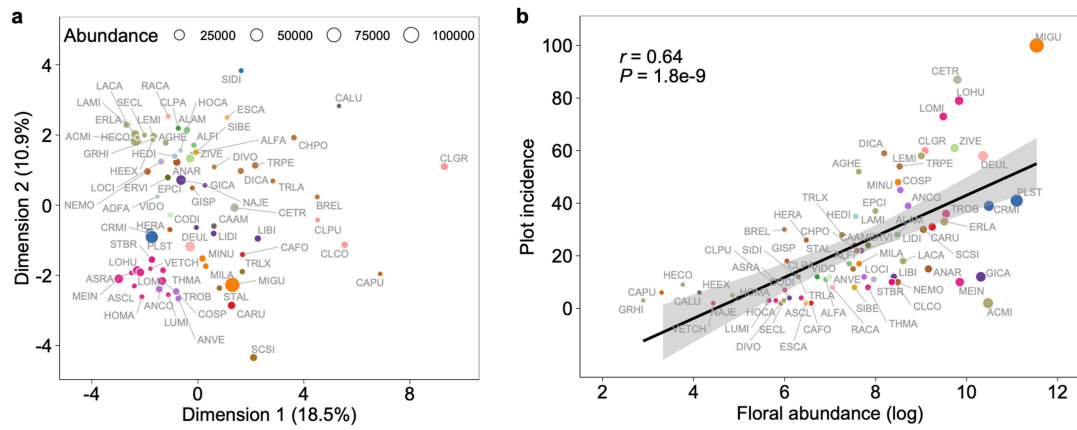
Extended Data Fig. 1 | Community-wide plant-pollinator network. a, Plant species ($n = 79$) coloured by families are arranged on the left according to phylogeny. The numbers of pollinator species that plants interacted with are shown as black bars and numbers within parentheses. **b,** Pollinator species

($n = 416$) are arranged along the top according to the size and similarity of plant assemblages that they interacted with. **c,** The observed numbers of interactions are denoted as frequency ('Freq') by the colour scale.



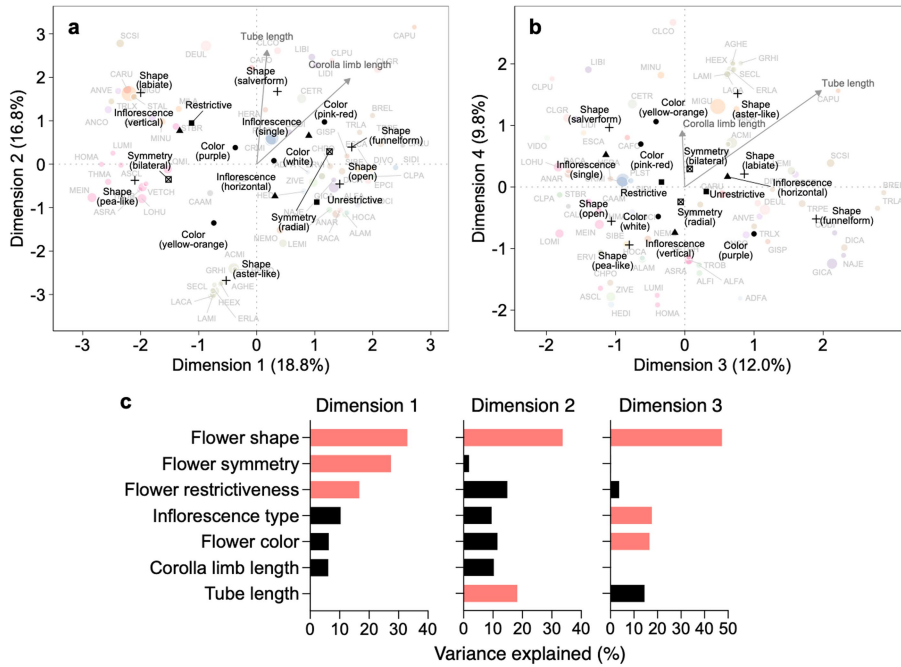
Extended Data Fig. 2 | Rarefaction shows that the majority of pollinator diversity was captured with our sampling intensity. Rarefaction curves of each of the 79 plant species (a, b) that were observed for plant–pollinator interactions (Supplementary Table 1) and the 64 plant species (c, d) that were included in the phylogenetic structural equation models (Fig. 2). The observed number of pollinators is represented by the solid portion of each coloured line,

whereas the dashed portion indicates extrapolation in the rarefaction analysis using the R package iNEXT⁴². Lines colours are randomly assigned. Pollinator diversity, especially Chao’s Shannon diversity (b, d), started to level off at the observed number of pollinators for most plant species, reflecting sufficient sampling to capture pollinator diversity.



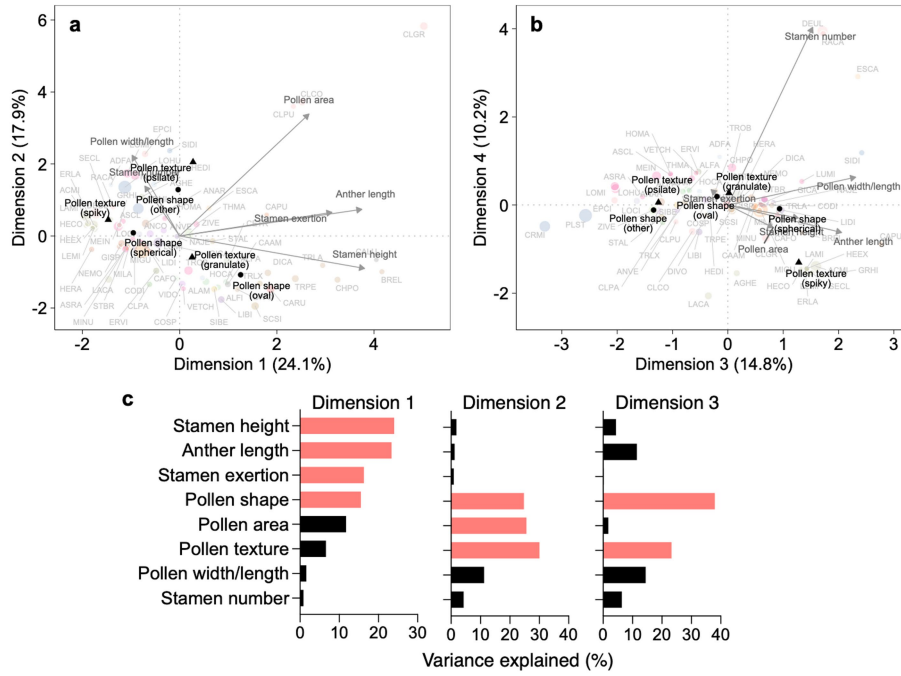
Extended Data Fig. 3 | Floral trait variation and abundance. a. Multivariate analysis (factor analysis of mixed data, FAMD) of 20 floral traits (Supplementary Table 3). Plant species ($n = 73$, abbreviated as the first two letters of genus and species names and coloured by plant family) are segregated along the first two dimensions, representing mainly size-related and other (shape/colour/inflorescence) floral traits, respectively. These traits

vary independently from species floral abundance (symbol size). **b.** Species rarity based on floral abundance (log-transformed) was correlated with rarity based on occurrence in the number of surveyed plots (see Methods, two-sided Pearson's correlation test, $r = 0.64$, $t = 6.9$, $d.f. = 70$, $P = 1.8 \times 10^{-9}$). The 95% confidence intervals of the mean are shown.



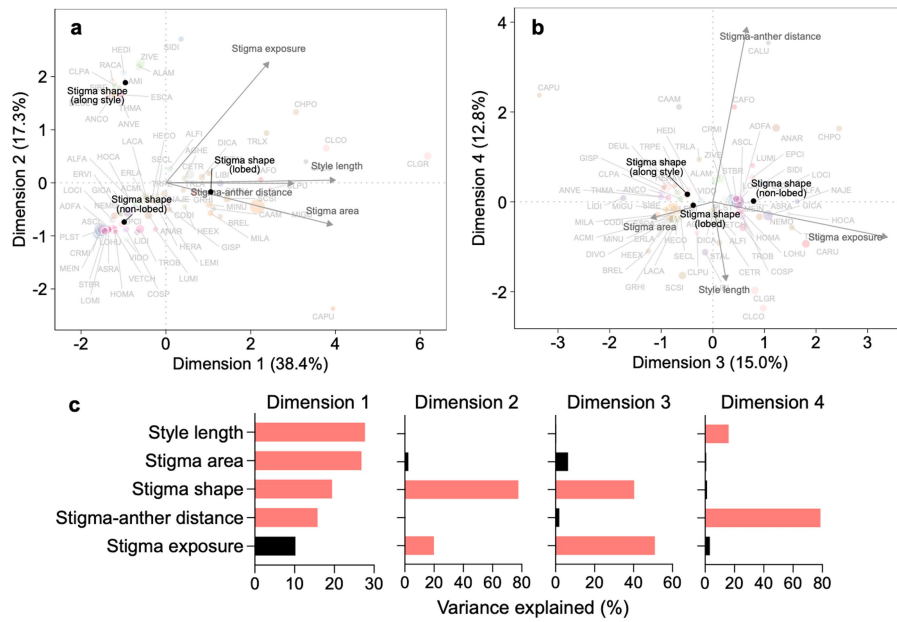
Extended Data Fig. 4 | Multivariate analysis of floral traits associated with pollinator attraction. **a, b**, In the first four dimensions of the factor analysis of mixed data (FAMD), the centroid of each category within a qualitative trait is indicated, with symbol shape representing different qualitative traits. Quantitative traits are represented by arrows. Individual plant species ($n = 73$)

are shown in the background with colours indicating plant families and symbol sizes indicating floral abundances (Extended Data Fig. 3). **c**, The traits that contributed to $\geq 15\%$ of variation of the first three dimensions are highlighted in colour.



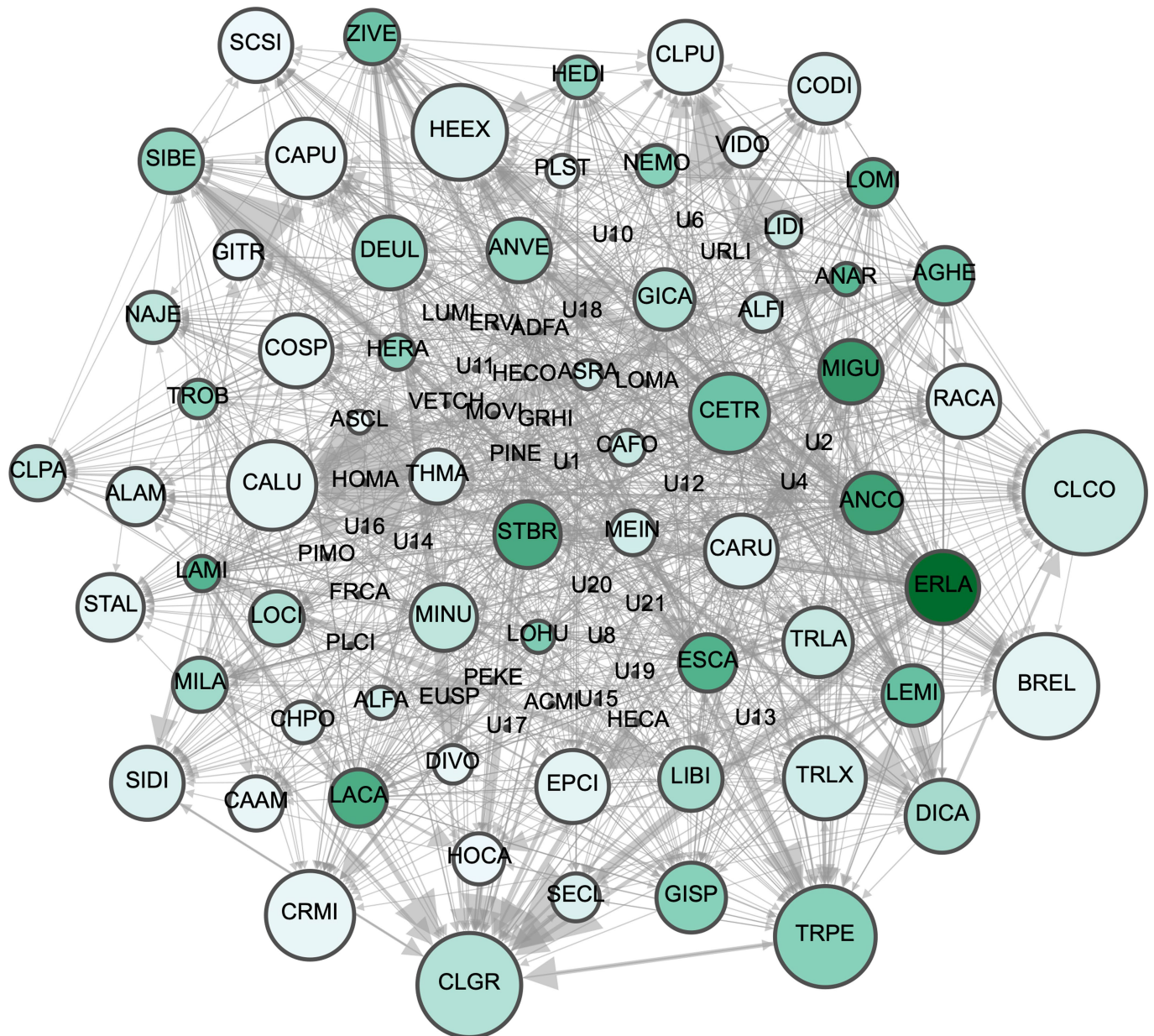
Extended Data Fig. 5 | Multivariate analysis of floral traits associated with male organ. a, b, In the first four dimensions of the factor analysis of mixed data (FAMD), the centroid of each category within a qualitative trait is indicated, with symbol shape representing different qualitative traits. Quantitative traits are represented by arrows. Individual plant species ($n = 73$)

are shown in the background with colours indicating plant families and symbol sizes indicating floral abundances (Extended Data Fig. 3). **c,** The traits that contributed to $\geq 15\%$ of variation of the first three dimensions are highlighted in colour.



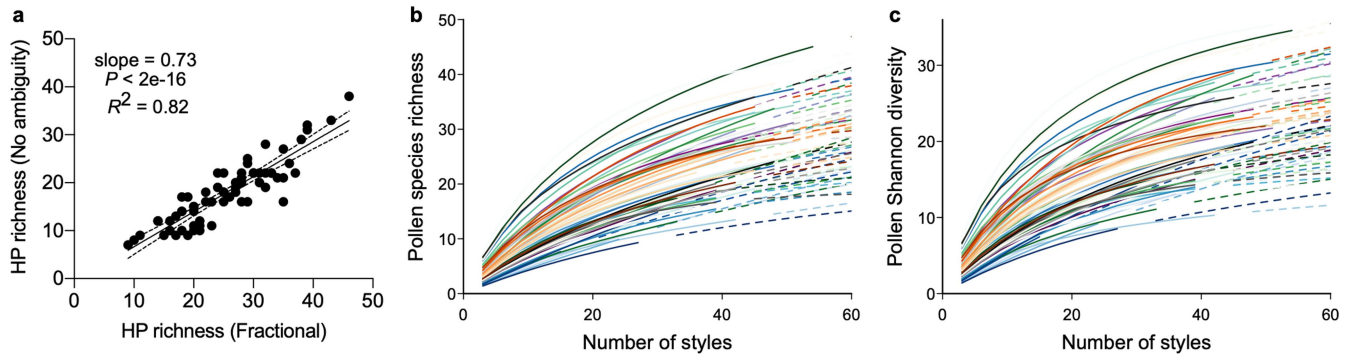
Extended Data Fig. 6 | Multivariate analysis of floral traits associated with female organ. **a, b**, In the first four dimensions of the factor analysis of mixed data (FAMD), the centroid of each category within a qualitative trait is indicated, with symbol shape representing different qualitative traits. Quantitative traits are represented by arrows. Individual plant species ($n = 73$)

are shown in the background with colours indicating plant families and symbol sizes indicating floral abundances (Extended Data Fig. 3). **c**, The traits that contributed to $\geq 15\%$ of variation of the first four dimensions are highlighted in colour.



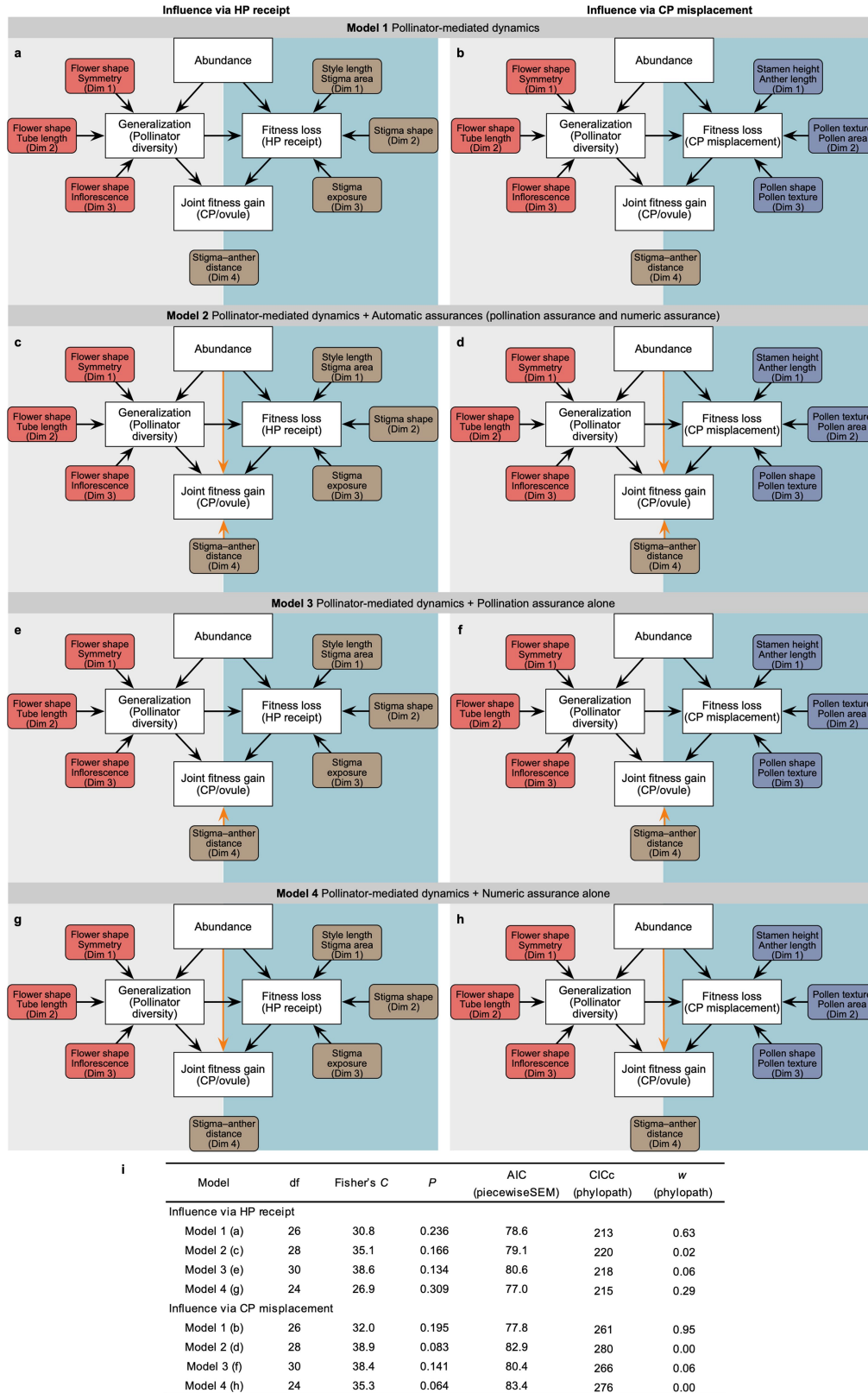
Extended Data Fig. 7 | Pollen transfer network. The network was constructed based on pollen deposited on 54 stigmas of 66 individual plant species (Supplementary Table 5). Plant species (nodes) are abbreviated as the first two letters of genus and species names (Supplementary Table 3), with unidentified species denoted with 'U'. Node size indicates the number of flowering plant

species that pollen is received from, and node colour darkness indicates the number of flowering plant species that pollen is donated to. That is, larger nodes represent better recipients and darker nodes better donors. Arrows and their sizes indicate the direction and amount (counts) of pollen transfer, respectively.



Extended Data Fig. 8 | Validation of fractional identity approach and rarefaction of pollen received by stigmas. **a**, There was a strong relationship between heterospecific pollen (HP) richness when fractionally identified pollen grains were excluded (y-axis, 'no ambiguity') and included (x-axis, 'fractional'): $n = 66$ plant species, general linear model, slope = 0.73, $t = 17.1$, $P < 2 \times 10^{-9}$. The dotted 95% confidence intervals of the mean are shown.

b, c, Rarefaction analysis using the R package iNEXT⁴² showed that the majority of pollen species richness (**b**) and Chao's Shannon diversity (**c**) were captured by the sampled styles ($n = 54$ on average) for each plant species ($n = 66$, coloured lines). The observed (solid) and extrapolated (dashed) portion of each rarefaction line are indicated.



Extended Data Fig. 9 | Phylogenetic structural equation models (PSEMs). **a-h**, The PSEMs considered pollinator niche partitioning, asymmetric facilitation, pollination assurance and numeric assurance (orange arrows). Pollination assurance and numeric assurance are collectively referred to as automatic assurances. **i**, Model fitting and nested model selection used the R

packages piecewiseSEM⁷⁰ and phylopath⁷⁴. Sample size was 64 plant species. *df* and *P*, degree of freedom and *P* value of the two-sided Fisher's *C* statistic; AIC, the Akaike's information criterion; CICc, the *C* statistic information criterion corrected for small sample sizes; *w*, CICc weights. Standardized regression coefficients of paths and model averaging are in Supplementary Table 6.

Extended Data Table 1 | Serpentine seep system within the McLaughlin Natural Reserve study area

Seep	Seep name	Latitude	Longitude	Seep area (m ²)	Number of survey plots in 2016	Number of survey plots in 2017
BS	Banana Slug	38.8622°N	122.3992°W	2200	13*	13
RHA	Research Hill A	38.8589°N	122.4103°W	2200	12	11
RHB	Research Hill B	38.8572°N	122.4075°W	2200	16	15
TPW	Tailings Pond West	38.8661°N	122.4511°W	2300	11	11
TP9	Tailings Pond Site 9	38.8639°N	122.4272°W	1300	9*	8

Pollinators, floral abundances and styles were surveyed and collected across this system. Within each seep, floral abundances were recorded 9* to 10 times each year across 8–16 1 m × 3 m plots per seep, depending on seep size and flowering duration.

Reporting Summary

Nature Portfolio wishes to improve the reproducibility of the work that we publish. This form provides structure for consistency and transparency in reporting. For further information on Nature Portfolio policies, see our [Editorial Policies](#) and the [Editorial Policy Checklist](#).

Statistics

For all statistical analyses, confirm that the following items are present in the figure legend, table legend, main text, or Methods section.

n/a Confirmed

- The exact sample size (n) for each experimental group/condition, given as a discrete number and unit of measurement
- A statement on whether measurements were taken from distinct samples or whether the same sample was measured repeatedly
- The statistical test(s) used AND whether they are one- or two-sided
Only common tests should be described solely by name; describe more complex techniques in the Methods section.
- A description of all covariates tested
- A description of any assumptions or corrections, such as tests of normality and adjustment for multiple comparisons
- A full description of the statistical parameters including central tendency (e.g. means) or other basic estimates (e.g. regression coefficient) AND variation (e.g. standard deviation) or associated estimates of uncertainty (e.g. confidence intervals)
- For null hypothesis testing, the test statistic (e.g. F , t , r) with confidence intervals, effect sizes, degrees of freedom and P value noted
Give P values as exact values whenever suitable.
- For Bayesian analysis, information on the choice of priors and Markov chain Monte Carlo settings
- For hierarchical and complex designs, identification of the appropriate level for tests and full reporting of outcomes
- Estimates of effect sizes (e.g. Cohen's d , Pearson's r), indicating how they were calculated

Our web collection on [statistics for biologists](#) contains articles on many of the points above.

Software and code

Policy information about [availability of computer code](#)

Data collection

Data analysis

For manuscripts utilizing custom algorithms or software that are central to the research but not yet described in published literature, software must be made available to editors and reviewers. We strongly encourage code deposition in a community repository (e.g. GitHub). See the Nature Portfolio [guidelines for submitting code & software](#) for further information.

Data

Policy information about [availability of data](#)

All manuscripts must include a [data availability statement](#). This statement should provide the following information, where applicable:

- Accession codes, unique identifiers, or web links for publicly available datasets
- A description of any restrictions on data availability
- For clinical datasets or third party data, please ensure that the statement adheres to our [policy](#)

All data that support the findings of this study are included in this published article and its supplementary information files and source data files.

Field-specific reporting

Please select the one below that is the best fit for your research. If you are not sure, read the appropriate sections before making your selection.

- Life sciences Behavioural & social sciences Ecological, evolutionary & environmental sciences

For a reference copy of the document with all sections, see nature.com/documents/nr-reporting-summary-flat.pdf

Ecological, evolutionary & environmental sciences study design

All studies must disclose on these points even when the disclosure is negative.

Study description

The study consisted of field observations of plant–pollinator interactions and collection of insect pollinators for taxonomic identification, field survey of floral abundance, collection of flowers for floral trait measurements, and collection of styles for stigma pollen identification. The study was carried out in the co-flowering community of the species-rich serpentine seep system at the McLaughlin Natural Reserve in California, USA (38.8582°N, 122.4093°W). In this system, field work was conducted in fives seeps separated by 0.3–5 km. Each seep (area = 1300 – 2300 square meters; Extended Data Table 1) was visited once every week during the peak of flowering season (April–June) for a total of 9 to 10 weeks each year in 2016 and 2017.

Research sample

The observations of plant–pollination interactions were conducted between 0800–1700 h by two to three persons simultaneously and extended to 1900 h for crepuscular flowers, once per week at each seep at McLaughlin Natural Reserve in California, USA. Across seeps and both years (2016 and 2017), insect pollinators that visited the 79 co-flowering plant species were captured and identified to the lowest taxonomic level possible (typically species level). As we aimed to collect an equal number of pollinators per plant species ($n = 150$ on average) evenly across seeps and years, each plant species was observed for 20–30 min per day. More time was invested (1–2 hours per day) observing plants that were infrequently visited. Despite additional time invested, it did not yield more pollinator observations for some species, including the ones that flowered in the evening (e.g. *Linanthus dichotomus*) or had exceptionally small flowers (e.g. *Hesperolinin californicum*, *Heterocodon rariflorus*, *Githopsis specularioides*).

For 73 out of the 79 co-flowering plant species, we scored 20 floral functional traits, including seven attraction traits, eight male organ traits, and five female organ traits for each plant species (Supplementary Table 3).

To identify pollen deposition on stigmas, three styles (from different individuals) per species were collected from spent flowers on the same day as pollinator observations. From this vast collection, we used a stratified random subsampling across all seeps and both years to achieve 90 (18 × 5) date–seep combinations, and a total of 54 styles per species for stigma pollen identification, and 14 species (Supplementary Methods) were excluded because they did not meet the sampling goals. In total, we taxonomically identified 3.1 million pollen grains.

Floral abundance survey was conducted weekly in fixed plots (1 m × 3 m each) at each seep in both years. Plots ($n = 8–16$ each site; Extended Data Table 1) were positioned along the length of each seep 1–20 m apart to capture plant species diversity within a site.

Sampling strategy

For plant species, we focused on all the 79 co-flowering plant species within the seeps in the two years. This represents a complete sampling of the animal-pollinated plants within the seeps, so no statistical test was run to determine the sample size.

For pollinator observations, we aimed to collect an equal number of pollinators per plant species ($n = 150$ on average). We used the rarefaction analysis to confirm that our sampling effort captured the majority of pollinator diversity for each of the 79 plant species (Extended Data Fig. 2a, b), especially for the plant species ($n = 64$, Extended Data Fig. 2c, d) that were included in the downstream phylogenetic structural equation modeling.

For style collections for stigma pollen identification, we used the rarefaction analysis to confirm that our sampling effort of styles ($n = 54$ per species on average) captured the majority of heterospecific donor species for each recipient plant species (Extended Data Fig. 8).

Data collection

Pollinator observation and collection and floral abundance survey were conducted by eye by R.L.K., E.M.O., R.A.H., G.A.-G., and T.-L.A. Floral functional traits were taken by R.L.K., R.A.H., and research assistants (see Acknowledgements). Floral traits were measured with a digital caliper (± 0.1 mm), Leica DM500 microscope, dissecting microscope, ImageJ v1.47, and/or visual inspection. Pollen grains were identified by R.L.K., E.M.O., R.A.H., and research assistants (see Acknowledgements) using a Leica DM500 microscope (Leica Microsystems, Wetzlar, Germany). Pinned or ethanol preserved insect pollinator specimens were identified by experts using eye and stereomicroscopes (Leica EZ4 W): bees (Anthophila) by Jaime Pawelek (Wild Bee Garden Designs), beetles (Coleoptera) by Robert Androw (Carnegie Museum of Natural History, Pittsburgh, PA), flies (Diptera) by Ben Coulter (Carnegie Museum of Natural

History, Pittsburgh, PA), and moths and butterflies (Lepidoptera), as well as remaining insects, by John Rawlins (Carnegie Museum of Natural History, Pittsburgh, PA).

Timing and spatial scale Data were collected across five seeps (separated by 0.3–5 km; total area = 1300 – 2300 square meters; Extended Data Table 1) during the peak of flowering season (April–June) over two years in 2016 and 2017. Each seep was visited once every week for a total of 9 to 10 weeks each year. The study captured the major flowering periods across the herbaceous, non-graminoid species, and ceased when flowering was tapering off for the majority of species in these seeps (Supplementary Table 3).

Data exclusions Because we aimed for a total of 54 styles per species for stigma pollen identification, 14 species (*Achillea millefolium*, *Aquilegia eximia*, *Castilleja attenuata*, *Dichelostemma congestum*, *Eriogonum vimineum*, *Grindelia hirsutula*, *Hesperolinon californicum*, *Hemizonia congesta*, *Lomatium macrocarpum*, *Lupinus microcarpus*, *Micropus californicus*, *Microseris douglasii*, *Minuartia douglasii*, and *Vicia sativa*) did not meet our sampling goals (mean = 54 styles per species, minimum = 36 styles per species, Supplementary Table 5) and were excluded from downstream interspecific pollen transfer network and phylogenetic structural equation modeling. This was described in Supplementary Methods.

Reproducibility The data were collected during the field study over two years, and were not repeated as in experiments. We described the methods of data collection and analyses in detail, allowing the work to be repeated.

Randomization The order of visiting different seeps for field data collection was randomized each week. Within each seep, the fixed plots for surveying floral abundances were randomly placed along the length of each seep to capture plant species diversity. To select styles ($n = 54$ per species on average) for stigma pollen identification, we used a stratified random subsampling across all seeps and both years to achieve 90 (18×5) date–seep combinations.

Blinding Blinding was not relevant to our field study because it was observational in nature. Although samples were not blinded, components of the study were collected by different team members who did not have knowledge of the associated data.

Did the study involve field work? Yes No

Field work, collection and transport

Field conditions Field data collection was conducted between 0800–1700 h each day and were extended to 1900 h for two species with crepuscular flowers (*Linanthus dichotomus* and *Chlorogalum pomeridianum*), during the peak of flowering season (April–June) in the serpentine seep system.

Location The serpentine seep system is at the McLaughlin Natural Reserve in California, USA (38.8582°N, 122.4093°W; see also Extended Data Table 1).

Access & import/export Permissions to access seeps, conduct research and to collect insect and plants were granted by the McLaughlin Natural Reserve (UCNRS #30941) April 6, 2015

Disturbance The seeps and organisms were not disturbed by other means than the sampling.

Reporting for specific materials, systems and methods

We require information from authors about some types of materials, experimental systems and methods used in many studies. Here, indicate whether each material, system or method listed is relevant to your study. If you are not sure if a list item applies to your research, read the appropriate section before selecting a response.

Materials & experimental systems

- n/a Involved in the study
- Antibodies
- Eukaryotic cell lines
- Palaeontology and archaeology
- Animals and other organisms
- Human research participants
- Clinical data
- Dual use research of concern

Methods

- n/a Involved in the study
- ChIP-seq
- Flow cytometry
- MRI-based neuroimaging

Animals and other organisms

Policy information about [studies involving animals](#); [ARRIVE guidelines](#) recommended for reporting animal research

Laboratory animals No laboratory animals were used in the study.

Wild animals Insects visiting a plant species were collected with a sweep net, chilled and then preserved. Lepidopteran insects were preserved dry, and non-Lepidopteran insects were euthanized and preserved with 100% ethanol in a -20 °C freezer and transported on ice to the laboratory at the University of Pittsburgh, where they were pinned and later sent out for taxonomic identification by experts.

Only Hymenoptera were identified by sex (males = 841, females = 4108).

Field-collected samples

The vast majority of preserved insect specimens were deposited at the Carnegie Museum of Natural History (Pittsburgh, PA), and a small subset of was kept by Jaime Pawelek (Wild Bee Garden Designs). No live animals were retained.

Ethics oversight

The study did not require ethical oversight.

Note that full information on the approval of the study protocol must also be provided in the manuscript.